Journal of Translational Medicine

RESEARCH

Open Access

LINC01116-dependent upregulation of RNA polymerase I transcription drives oncogenic phenotypes in lung adenocarcinoma

Shashanka Shekhar Sarkar[1], Mansi Sharma[1†], Sheetanshu Saproo[1†] and Srivatsava Naidu[1*]

Abstract

Background Hyperactive RNA Polymerase I (Pol I) transcription is canonical in cancer, associated with malignant proliferation, poor prognosis, epithelial-mesenchymal transition, and chemotherapy resistance. Despite its significance, the molecular mechanisms underlying Pol I hyperactivity remain unclear. This study aims to elucidate the role of long noncoding RNAs (lncRNAs) in regulating Pol I transcription in lung adenocarcinoma (LUAD).

Methods Bioinformatics analyses were applied to identify lncRNAs interacting with Pol I transcriptional machinery. Fluorescence in situ hybridization was employed to examine the nucleolar localization of candidate lncRNA in LUAD cells. RNA immunoprecipitation assay validated the interaction between candidate lncRNA and Pol I components. Chromatin isolation by RNA purification and Chromatin Immunoprecipitation (ChIP) were utilized to confirm the interactions of candidate lncRNA with Pol I transcriptional machinery and the rDNA core promoter. Functional analyses, including lncRNA knock-in and knockdown, inhibition of Pol I transcription, quantitative PCR, cell proliferation, clonogenicity, apoptosis, cell cycle, wound-healing, and invasion assays, were performed to determine the effect of candidate lncRNA on Pol I transcription and associated malignant phenotypes in LUAD cells. ChIP assays and luminometry were used to investigate the transcriptional regulation of the candidate lncRNA.

Results We demonstrate that oncogenic LINC01116 scaffolds essential Pol I transcription factors TAF1A and TAF1D, to the ribosomal DNA promoter, and upregulate Pol I transcription. Crucially, LINC01116-driven Pol I transcription activation is essential for its oncogenic activities. Inhibition of Pol I transcription abrogated LINC01116-induced oncogenic phenotypes, including increased proliferation, cell cycle progression, clonogenicity, reduced apoptosis, increased migration and invasion, and drug sensitivity. Conversely, LINC01116 knockdown reversed these effects. Additionally, we show that LINC01116 upregulation in LUAD is driven by the oncogene c-Myc, a known Pol I transcription activator, indicating a functional regulatory feedback loop within the c-Myc-LINC01116-Pol I transcription axis.

Conclusion Collectively, our findings reveal, for the first time, that LINC01116 enhances Pol I transcription by scaffolding essential transcription factors to the ribosomal DNA promoter, thereby driving oncogenic activities in LUAD. We propose the c-Myc-LINC01116-Pol I axis as a critical oncogenic pathway and a potential therapeutic target for modulating Pol I transcription in LUAD.

Keywords RNA polymerase I transcription, SL1, Pol I transcription in cancer, Transcriptional regulation in cancer, Long non-coding RNAs, Lung adenocarcinoma, LINC01116, EMT, Chemoresistance

†Mansi Sharma and Sheetanshu Saproo have equal contribution.

*Correspondence:
Srivatsava Naidu
srivatsava.naidu@iitrpr.ac.in

Graphical Abstract

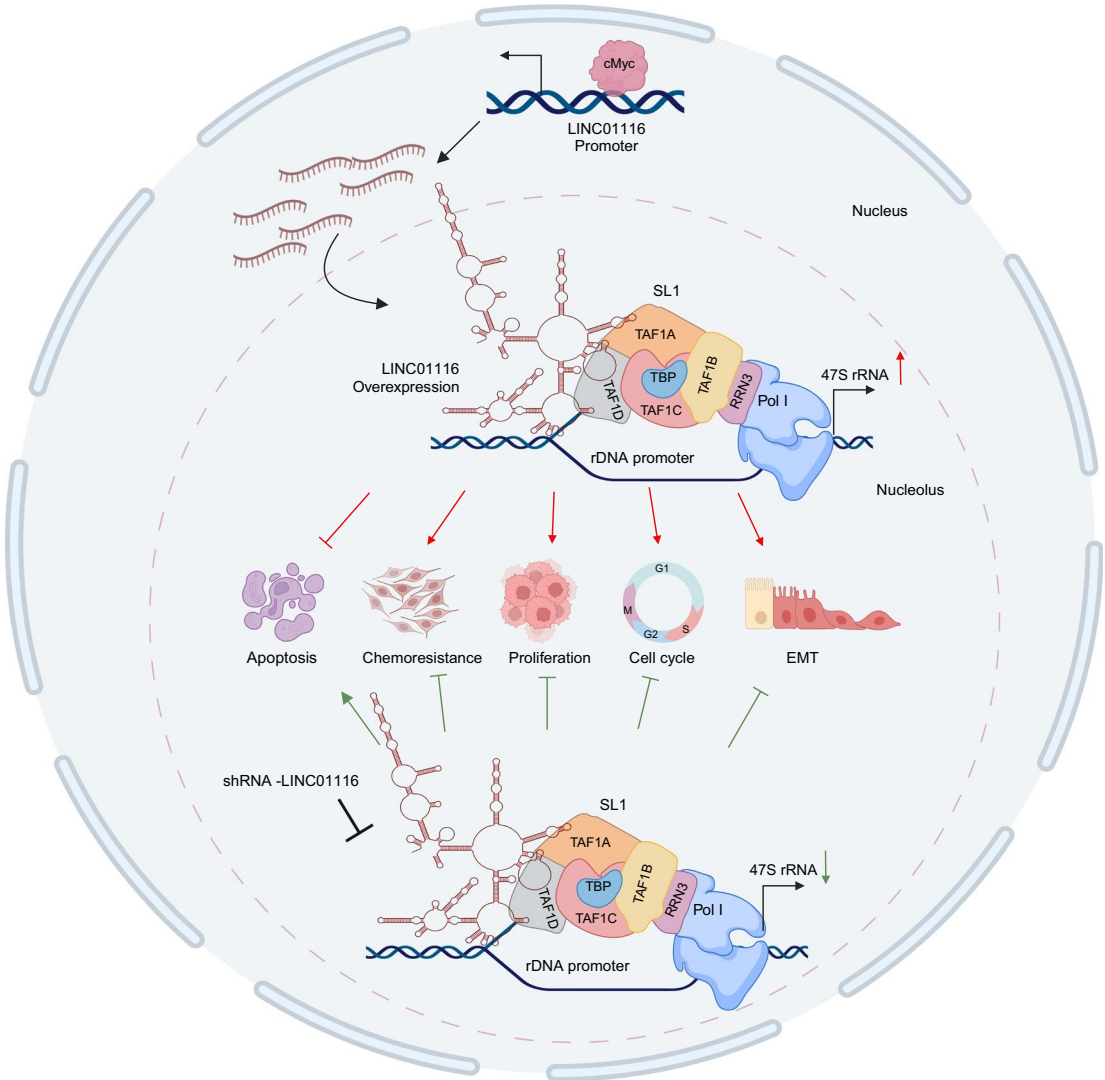

Introduction

The transcription of ribosomal DNA (rDNA) into ribosomal RNA (rRNA) by RNA Polymerase I (Pol I) is a rate-limiting step in ribosome biogenesis, directly affecting cellular translational capacity, thus influencing growth, proliferation, differentiation, and apoptosis [1]. Hyperactive Pol I transcription, often accompanied by upregulation of its core transcriptional machinery, is a molecular anomaly frequently observed in diverse cancer types [2]. Moreover, a multitude of epigenetic alterations within the rDNA loci have been implicated in oncogenic processes [3]. Recently, a specific N6-methyladenosine modification in 18S rRNA has shown to promote tumorigenesis and chemoresistance [4]. Notably, heightened Pol I transcription has been associated with adverse prognosis [5, 6], therapeutic resistance [7], and epithelial-mesenchymal transition (EMT) [8]. These findings underscore the indispensable role of hyperactive Pol I transcription in driving oncogenic processes.

The initiation of Pol I transcription is orchestrated by class-specific machinery, including Selectivity Factor 1 (SL1), a complex of TATA-binding protein (TBP) and four TBP-associated factors (TAFs—TAF1A, TAF1B, TAF1C, and TAF1D), Upstream Binding Factor (UBF), RRN3, and Pol I enzyme [9]. These core components assemble at the rDNA promoter to form the

pre-initiation complex (PIC), a crucial step for initiating transcription. Remarkably, these protein–protein and protein-rDNA interactions are direct targets of signaling circuitry governing cell growth and proliferation [10]. Oncoprotein c-Myc stimulates PIC-rDNA promoter interactions primarily through Ras/MAPK, PI3K, and mTOR pathways [11]. Meanwhile, tumor suppressors such as pRb and p53 restrain PIC activity [11–13]. Oncogenic aberrations disrupting this balance amplify PIC activity on the rDNA promoter, resulting in unrestrained rRNA synthesis critical for malignant proliferation [14]. Recently, we reported a novel microRNA-circularRNA-mediated post-transcriptional mechanism contributing to the upregulation of Pol I transcription in lung adenocarcinoma (LUAD) [15]. However, the intricate molecular mechanisms, particularly those involving regulatory RNAs, contributing to the hyperactivation of Pol I transcription in cancer, remain largely elusive.

Long noncoding RNAs (lncRNAs), a class of regulatory RNAs, are integral to modulating gene expression programs. LncRNAs exert their functions through diverse interactive mechanisms, including molecular scaffolding, decoying, competitive binding, and epigenetic modulation [16]. These multifaceted interactions of lncRNAs with cellular proteins and nucleic acids profoundly influence crucial cellular processes, including growth, proliferation, apoptosis, and cell fate determination in health and disease. Accumulating evidence revealed that lncRNAs exhibit dual roles as drivers of both tumor suppression and oncogenesis across various cancer types, underscoring their intricate role in the regulatory landscape of cancer [17].

Recent studies have identified LINC01116 as significantly upregulated in various cancers, playing an oncogenic role in several cancer hallmarks and contributes to therapeutic resistance [18–20]. However, the underlying mechanisms through which LINC01116 exerts its oncogenic effects remain largely unclear. This study unveils a novel oncogenic mechanism of LINC01116 through Pol I transcription. We demonstrated that LINC01116 enhances Pol I transcription by directly binding to the rDNA promoter and promoting PIC assembly in LUAD cell lines. Notably, LINC01116-dependent activation of Pol I transcription is vital for its oncogenic function. Inhibition of Pol I transcription mitigated LINC01116-induced tumor promoting processes. Furthermore, we identified c-Myc as a driver of LINC01116 upregulation in LUAD. These findings underscore the c-Myc-LINC01116-Pol I axis as a novel oncogenic pathway and propose LINC01116 as a potential therapeutic target for modulating Pol I transcription-mediated oncogenic phenotypes in LUAD.

Materials and methods

All the primers, probes, and antibodies used in the study are listed in Additional file 1: Table S1.

In-silico analysis

Interactions between lncRNAs and Pol I transcriptional machinery were predicted using RNAct [21], SFPEL-LPI [22], and catRAPIDomics [23]. The Cancer Genome Atlas (TCGA) LUAD RNA-sequencing data was analyzed using RNAInter (www.rnainter.org) to predict LINC01116 interactors, which were then subjected to Gene Set Enrichment Analysis (GSEA) using GSEA v4.2.3 application available on molecular signatures database MSigDB (www.gsea-msigdb.org/gsea/index.jsp). RNA-sequencing data for LINC01116 and c-Myc in LUAD were retrieved from TCGA and Clinical Proteomic Tumor Analysis Consortium (CPTAC) using cBioPortal (https://www.cbioportal.org/) and analysed for correlation. Putative c-Myc binding sites on the LINC01116 promoter were predicted using the LASAGNA application (https://biogrid-lasagna.engr.uconn.edu).

Molecular cloning

The full-length transcript of LINC01116 was PCR amplified using gene-specific cloning primers and cloned into MluI and BamHI restriction sites of pCMV6 expression vector (Origene, Rockville, Maryland, USA). Sense and anti-sense shRNA oligos targeting nucleotides 201-221 of LINC01116 were synthesized (Eurofins, Bangalore, India), and oligo ends were phosphorylated using T4 polynucleotide kinase (Invitrogen), annealed and cloned into AgeI and EcoRI restriction sites of pLKO.1 puro expression vector (#8453 Addgene, Watertown, MA, USA) as per Addgene protocol. LINC01116 promoter region was PCR-amplified from human genomic DNA (Promega) and cloned into MluI and KpnI restriction sites of pGL3-basic vector (Promega). Insert sequences were confirmed by Sanger sequencing.

Cell culture and transfections

A549, H23, and HEK293T cells were purchased from the National Centre for Cell Science, Pune, India. Cells were authenticated at source by short tandem repeat analysis and monitored for Mycoplasma contamination. Cells were maintained in RPMI 1640 medium (A549 and H23) or DMEM (HEK293T) (Gibco, Thermo Fisher Scientific, Waltham, MA, USA), supplemented with 10% fetal bovine serum (FBS) (Gibco) and 100 U/mL penicillin–streptomycin (Gibco, Thermo Fisher Scientific) at 37 °C and 5% CO_2 in a humidified incubator (Forma Steri-Cycle i60, Thermo Fisher Scientific). Cells were transfected with pCMV6 empty vector (eV) or pCMV6-LINC01116 expression vector using Lipofectamine 2000

(Invitrogen). To generate LINC01116-overexpressing stable cell lines, A549 and H23 cells were transfected with 1 µg of pCMV6-eV or pCMV6-LINC01116 using Lipofectamine 2000. After 48 h, cells were cultured in selection media containing 1000 µg/ml G418 (Roche, Sigma-Aldrich, St. Louis, MO, USA) until individual colonies formed. For stable LINC01116-shRNA transfection, A549 and H23 cells were transfected with 1 µg of pLKO.1-eV or LINC01116-shRNA, followed by clone selection using media containing 1 µg/mL Puromycin (Roche). For reconstitution of LINC01116 expression, LINC01116 stable knockdown cells were transiently transfected with pCMV6-LINC01116 expression vector using Lipofectamine 2000.

RNA isolation and quantitative real-time PCR

Total RNA from cells was isolated using TRIzol (Ambion, Thermo Fisher Scientific) according to the manufacturer's protocol, and reverse transcribed using High-Capacity cDNA reverse transcription kit (Applied Biosystems, Thermo Fisher Scientific). The quantitative real-time PCR (qPCR) was performed using SYBR green chemistry (Applied Biosystems) on Quant Studio 5 qPCR system (Applied Biosystems, Thermo Fisher Scientific). For gene expression analysis, Gamma-Actin, or small nuclear RNA U6 were used as internal controls.

LUAD RNA samples

RNA isolated from LUAD or adjacent normal samples were purchased from the National Cancer Tissue Bank at the Indian Institute of Technology Madras, Chennai, India.

RNA Immunoprecipitation

RNA immunoprecipitation (RIP) was performed as previously [24]. Briefly, 1×10^6 A549 cells or A549 or H23 cells stably overexpressing LINC01116 or LINC01116-shRNA were cultured in a 10 cm dish for 24 h and cross-linked using 1% formaldehyde (Sigma-Aldrich), and the cross-linking was quenched using glycine (final concentration of 0.25 M). Next, cells were washed twice with 1X DPBS and, resuspended in lysis buffer, and sonicated at 32% amplitude and 15 cycles with 30 s on/off using Sinaptec ultrasonicator (Lezennes, France) and subjected to DNase (Invitrogen) treatment (250 U/mL) for 30 min at 37 °C. For immunoprecipitation, Protein A beads (Invitrogen) were bound to either IgG isotype control or TAF1A or TAF1D antibodies, followed by incubation with DNase-treated cell lysate supernatant. Next, the antibody-bound RNA and 1% Input samples were subjected to 18 µL Proteinase K (Invitrogen) treatment for 30 min at 55 °C. Total RNA was isolated using the TRIzol method, and LINC01116 association with TAF1A and TAF1D was validated using qPCR.

Fluorescence in-situ hybridization

Fluorescence in-situ hybridization (FISH) was performed as previously [25]. Briefly, 1×10^4 A549 cells stably overexpressing LINC01116 or LINC01116-shRNA were cultured overnight on coverslips in a 12 well plate. Cells were fixed with 3.7% formaldehyde for 10 min at room temperature (RT) and permeabilized with 70% ethanol for 1 h at RT. The fixed cells were probed with LINC01116-specific 6-FAM-tagged probe (Merck) at 8 nM concentration and incubated with NPM1/TAF1A/TAF1D primary antibody in hybridization buffer (20% formamide (Sigma-Aldrich), 0.02% RNAse-free BSA (Himedia Laboratories, India), 50 µg salmon sperm DNA (Sigma-Aldrich), 2X SSC in a humidified chamber at 37 °C and then incubated overnight in a dark chamber. Then, the cells were washed thrice with wash buffer and incubated with hybridization solution containing fluorescence-tagged secondary antibody in dark for 1 h at 37 °C. The cells were then counterstained with Hoechst 33342 (Invitrogen) and imaged using a fluorescence microscope (DMi8, Leica Microsystems, Wetzlar, Germany).

Nucleolar SL1 pulldown

Nucleolar SL1 pull-down was performed as previously [26], with minor modifications. Briefly, 1×10^6 A549 cells were cultured overnight in a 10 cm dish. Cells were cross-linked with 1% formaldehyde and quenched with 0.125 M Glycine for 10 min at RT. The cross-linked cells were lysed and sonicated (SinapTec Lab 120, France) to generate 100–600 bp DNA fragments. Sheared chromatin was immunoprecipitated with TAF1B antibody. Immunoprecipitated (IP) samples were aliquoted for Protein, Chromatin, and RNA isolation. The IP samples were eluted with 4X LDS sample buffer (Invitrogen) for protein isolation and proceeded for immunoblot. Sonicated chromatin was treated with RNase and Proteinase K, and subsequently, chromatin DNA was eluted using the QIAGEN PCR purification kit (QIAGEN). RNA was isolated using the Trizol method.

Chromatin immunoprecipitation

Chromatin immunoprecipitation (ChIP) assays were performed as described previously [27]. Briefly, 1×10^6 A549 cells stably expressing pCMV6-eV or pCMV6-LINC01116 or pLKO.1-eV or LINC01116-shRNA were cultured until 70% confluency in a 10 cm dish. Cells were cross-linked with 1% formaldehyde, and subsequently reaction was quenched using 0.125 M Glycine for 10 min at RT. The cross-linked cells were lysed and sonicated (32% amplitude for 15 cycles with 30 s on/off)

(SinapTec Lab 120, France) to generate 200–500 bp DNA fragments. For immunoprecipitation, IgG or, TAF1A or TAF1D or TAF1B or POLR1B antibodies were bound to Protein A magnetic beads for 3 h at RT, followed by incubation with sonicated chromatin. Bead-bound DNA–protein complexes were extracted using an extraction buffer (1% SDS, 0.1 M NaHCO3 and Protease inhibitor). The extracts were RNAse and Proteinase K treated sequentially, and ChIP DNA was eluted using QIAGEN PCR purification kit (QIAGEN). The relative enrichment of TAF1A, TAF1D, TAF1B, and POLR1B on the rDNA promoter was analyzed using qPCR.

Chromatin isolation by RNA purification

Chromatin isolation by RNA purification (ChIRP) was performed as described previously [28]. Briefly, 1×10^6 cells with stable overexpression of LINC01116 or A549 cells with stable knockdown of LINC01116 were cultured in 10 cm dish up to 70% confluency and cross-linked with 1% formaldehyde, and the cross-linking was quenched using 0.125 M glycine. Next, cells were lysed and sonicated at 32% amplitude for 15 cycles with 30 s on/off. The sonicated cell lysate was hybridized with biotinylated LINC01116 probe (Merck) in hybridization buffer for 4 h at RT. Next, the biotin probe-bound complexes were captured by streptavidin-conjugated magnetic beads (Biobharathi Life Sciences, India) and separated into two fractions. Each fraction was subjected to DNA elution or RNA elution with respective elution buffers, and the elutes were then treated with 5 µL Proteinase K (20 mg/mL) (Invitrogen) for 45 min at 50 °C. RNA was reverse transcribed and analyzed for LINC01116, and DNA was analyzed for rDNA using primers specific to the rDNA core promoter on qPCR. Further, the eluted DNA was PCR amplified and subjected to Sanger sequencing.

Ethynyl uridine incorporation assay

A549 or H23 cells stably overexpressing LINC01116 or LINC01116-shRNA were seeded in a 6-well plate at 1.5×10^5 cells/ well. After 48 h, the cells were incubated with 100 µM of ethynyl uridine (EU) (Sigma-Aldrich) for 1 h at 37 °C the dark. Next, the EU-labeled cells were cross-linked using 3.7% formaldehyde and permeabilized using 0.01% Triton-X 100. Next, the permeabilized cells were stained with 15 µM Azide fluor (Sigma-Aldrich). Stained cells were washed thrice with 1X phosphate-buffered saline, counterstained with Hoechst 33342 (Invitrogen), and imaged using a fluorescence microscope (Leica).

Cell proliferation assay

A549 or H23 cells stably overexpressing LINC01116 or LINC01116-shRNA were seeded at a density of 3000 cells/well in a 96-well plate. After overnight incubation, cells were then treated with 1 µM BMH-21 (Sigma-Aldrich), and control cells received DMSO. After 24 h, cells were incubated with the Alamar Blue Cell Viability Reagent (Invitrogen), and the absorbance was measured at 570 nm using a Clariostar plate reader (BMG Labtech, Ortenberg, Germany).

Cell cycle and apoptosis assays

A549 or H23 cells stably overexpressing LINC01116 or with stable knockdown of LINC01116 were cultured in a 6-well plate (1.5×10^5/well) and treated with BMH-21 (1 µM) for 24 h. Subsequently, cells were trypsinized and utilized for cell cycle and apoptosis assays. For cell cycle analysis, cells were fixed in 66.6% ice-cold ethanol at 4 ℃ for 2 h and then stained using the propidium iodide (PI) Flow Cytometry Kit (Abcam). For apoptosis analysis, cells were stained with the Annexin-V-PI Apoptosis Detection Kit I from BD Biosciences. Cells were analyzed on a BD C6 Plus flow cytometer (BD Biosciences, New Jersey, USA) and quantified using FlowJo software (BD Biosciences).

Scratch assay

A549 cells stably overexpressing LINC01116 or LINC01116-shRNA were seeded in a 6-well plate (1.5×10^5/well). Cells were treated with BMH-21 (1 µM). After 24 h, a scratch was made on the monolayer of cells and imaged at an interval of 24 h for a total of 72 h using an EVOS XL core light microscope (Invitrogen, Waltham, Massachusetts, USA).

Invasion assay

Matrigel (Corning, USA) was mixed at a 1:5 ratio with ice-cold serum-free media, 500 µL of this diluted Matrigel was applied to the upper section of a Transwell chamber and incubated at 37 °C for 2 h. Subsequently, BMH-21 treated A549 cells (1.5×10^5/well) stably overexpressing pCMV6-eV or pCMV6-LINC01116 or shRNA against LINC01116 introduced into the Matrigel-coated invasion chamber. Lower chamber of the well was filled with culture media containing 10% FBS, and incubated for 24 h. Later, the chambers were fixed using 100% ice-cold methanol for 15 min and stained with a 0.01% solution of crystal violet (Sigma-Aldrich) for 20 min at RT. Cells located on the upper side of the membrane were gently wiped off with a sterile cotton swab, and the remaining cells were visualized using a light microscope (Evos).

Clonogenicity assay

A549 or H23 cells stably overexpressing LINC01116 or with stable knockdown of LINC01116 were seeded in a six-well plate (10^3 cells/plate). The cells were treated with

BMH-21 and incubated in the humidified CO_2 incubator at 37 °C until the appearance of isolated colonies. The colonies were then fixed with 100% ice-cold methanol for 5 min and stained using 0.01% crystal violet (Sigma-Aldrich) solution for 20 min at RT. Colony images were manually captured and counted using ImageJ software.

Generation of A549 and H23 spheroids

Tumor cell spheroids were generated as previously [29]. Briefly, A549 or H23 cells stably overexpressing LINC01116 or LINC01116-shRNA were seeded in a 1×10^4/ well in agarose-coated 96-well plates cultured till the formation of visible spheroids. Spheroids were treated with 1 µM BMH-21 for 24 h. Next, the spheroids were analyzed for EU incorporation assay using the previously discussed protocol or processed for Ki-67 – immunofluorescence assay. Briefly, spheroids were fixed with 3.7% formaldehyde, blocked with 5% BSA for 1 h, and incubated with Ki67 primary antibody overnight, followed by fluorescence-tagged secondary antibody, and further counterstained with Hoechst 33342. The spheroids were imaged using a DMi8 fluorescence microscope (Leica).

Generation of cisplatin and doxorubicin resistant A549 cells

Cisplatin (Cis) and Doxorubicin (Dox) resistant A549 cells were generated by dose-escalation method. Drug treatment was initiated by culturing A549 cells with 1 µM Cis (Sigma-Aldrich) or 0.2 µM Dox (Sigma-Aldrich) for 48 h. Every month, apoptosis measurement was performed to assess the resistance development, and subsequently, the drug treatment was gradually increased to a final concentration of 10 µM Cis and 1 µM Dox. After six months of continuous exposure to Cis and Dox, drug resistance was validated by relative resistance to cell death compared with parental A549 cells.

Luciferase reporter assays

The dual luciferase assay was performed as previously [27]. Briefly, 1×10^5 HEK293T cells were seeded onto a 12-well plate and incubated overnight. Next, cells were co-transfected with 0.5 µg of pGL3 basic plasmid containing LINC01116-promoter construct, 0.5 µg of c-Myc (#16,011 Addgene), or 0.5 µg of eV and 50 ng of pRL-CMV (Promega) as an internal control using Lipofectamine 2000 (Invitrogen). 48 h post-transfection, cells were processed using Dual-Luciferase® Reporter Assay kit (Promega), and the luciferase activities were measured using GloMax® Navigator (Promega). The results were calculated by normalizing firefly luciferase to that of Renilla luciferase.

Statistics

All experiments were conducted with a minimum of three independent biological replicates. Results are depicted as the mean ± standard error of the mean (SEM). Statistical analysis was performed using GraphPad Prism (v. 8.2). Pearson analysis was employed for correlation assessment. A two-tailed Student's t-test was employed to compare the means between the two groups, multiple group comparisons were performed using one-way analysis of variance (ANOVA), followed by Tukey's post-hoc test. Results were considered statistically significant for p-values ≤ 0.05.

Results

LINC01116 directly interacts with transcriptionally active SL1 subunits TAF1A and TAF1D in the nucleolus

LncRNAs can regulate gene transcription by modulating the activity and recruitment of transcription factors [30, 31]. Since SL1 functions as an essential transcription factor and regulatory hub for Pol I transcription, we focused on identifying lncRNAs interacting with SL1 components. Utilizing multiple lncRNA-protein interaction tools, we identified LINC01116 as a high-confidence interactor with SL1 subunits TAF1A and TAF1D. LINC01116 demonstrated optimal binding affinity evidenced by catRAPIDomics star rating system, which integrates normalized interaction propensity, RNA/DNA binding domains, and known RNA binding motifs. Furthermore, LINC01116 was significantly upregulated in LUAD tissues, with elevated expression correlating with poor overall survival. This unique profile distinguished LINC01116 from other predicted lncRNAs, prioritizing it for functional characterization (Fig. 1A and Additional file 2, Figure S1). Strikingly, GSEA revealed a significant enrichment of LINC01116 target genes in pathways related to ribosome biogenesis (Fig. 1B, Additional file 3, Table S2) and rRNA metabolic processes (Fig. 1C, Additional file 4, Table S3). Further, using catRAPID fragments and graphic modules, we identified a specific binding region between TAF1A/TAF1D and LINC01116, spanning nucleotides 201–360 (Additional File 5, Figure S2). In addition, a significant positive correlation was observed between the expression of LINC01116 and 47S rRNA in LUAD tumors compared to adjacent normal tissues (Fig. 1D), suggesting a potential role of LINC01116 in Pol I transcription. LINC01116 and Pol I transcription are highly upregulated and associated with oncogenic roles in LUAD [15, 32]. Thus, we sought to investigate the regulatory link between LINC01116 and Pol I transcription in LUAD cell lines. To investigate the endogenous interaction between LINC01116 and TAF1A and TAF1D, we performed RIP assays in

A549 and H23 cells stably overexpressing LINC01116 (Fig. 1E) or LINC01116-shRNA (Fig. 1F). Remarkably, LINC01116 overexpression resulted in a substantial increase in TAF1A and TAF1D enrichment compared to controls. Conversely, knockdown of LINC01116 markedly diminished this enrichment, confirming the interaction between LINC01116 and, TAF1A and TAF1D (Fig. 1G and H). Pol I transcription is confined to the nucleolus [9]. We examined nucleolar localization of LINC01116 by immunofluorescence microscopy. Cells overexpressing LINC01116 exhibited a notable co-localization of LINC01116 along with TAF1A, TAF1D and the nucleolar marker NPM1 (Fig. 1I), which was diminished in LINC01116 knockdown cells (Fig. 1J). Transcriptionally competent TAF1A and TAF1D are integral components of the SL1 complex bound to rDNA promoter [33]. To test whether the interaction of LINC01116 is specific to the TAF1A/TAF1D subunits within the SL1 complex or free forms, we immunoprecipitated the SL1 complex bound to the rDNA-promoter and assessed the presence of SL1 components, LINC01116 and rDNA (scheme Fig. 1K). Immunoblotting analysis confirmed the presence of TAF1A-D, indicating successful isolation of the SL1 complex (Fig. 1L). Subsequent qPCR analysis of the Immunoprecipitated chromatin and RNA revealed significant enrichment of the rDNA core promoter (Fig. 1M) and LINC01116 (Fig. 1N). These findings strongly indicate the interaction between LINC01116 and TAF1A/TAF1D with transcriptionally competent SL1 complex bound to the rDNA promoter, suggesting a potential regulatory role for LINC01116 in Pol I transcription.

LINC01116 upregulates Pol I transcription by promoting pre-initiation complex formation at the rDNA promoter

To investigate whether LINC01116 affects PIC formation on the rDNA promoter, we performed ChIP assays with antibodies against PIC components. ChIP-qPCR analysis revealed a significant increase in SL1 components and POLR1B at the rDNA promoter upon LINC01116 overexpression (Fig. 2A). Conversely, LINC01116 knockdown significantly reduced this enrichment, indicating its critical role in recruiting PIC components to the rDNA promoter via TAF1A and TAF1D (Fig. 2B). LncRNAs can recruit transcription factors to regulatory sequences through direct DNA interactions [34]. Strikingly, alignment of the LINC01116 sequence with rDNA regulatory loci revealed a remarkable sequence complementarity between LINC01116 and the rDNA core promoter (+20 to -45) and the upstream control element (UCE) (-107 to -177) (Fig. 2C). To validate this, we conducted ChIRP assays. qPCR analysis of ChIRP-derived RNA and DNA fractions revealed a significant enrichment of both LINC01116 (Fig. 2D) and the rDNA core promoter (Fig. 2E) in LINC01116-overexpressing cells compared to controls. In contrast, stable knockdown of LINC01116 reversed the enrichment of both LINC01116 (Fig. 2F) and the rDNA core promoter (Fig. 2G). To further validate the sequence complementarity between LINC01116 and the rDNA promoter/UCE, we performed ChIRP-qPCR assays scanning the entire rDNA repeat. Notably, LINC01116 overexpression led to significant enrichment of core promoter and UCE, whereas LINC01116 knockdown resulted in reduced signals. In contrast, other regions of the rDNA repeat remained unaffected, highlighting the specificity of this interaction (Additional file 6, Figure S3). Sanger sequencing of the ChIRP DNA fraction confirmed the direct binding of LINC01116 to the rDNA core promoter (Fig. 2H). Next, we investigated the impact of LINC01116 on Pol I transcription by analyzing both steady-state levels and de novo synthesis of 47S pre-rRNA in cells with stable LINC01116 overexpression, knockdown, and reconstituted expression in knockdown cells (Fig. 2I). qPCR analysis revealed that LINC01116 overexpression elevated steady-state 47S rRNA levels, whereas knockdown resulted in decreased levels, notably, reconstitution of LINC01116 in knockdown cells significantly rescued 47S rRNA (Fig. 2J). Furthermore, EU incorporation assays demonstrated that LINC01116 overexpression enhanced de novo rRNA transcription, while knockdown reduced synthesis. Remarkably, reconstitution of LINC01116 in knockdown cells also restored de novo rRNA transcription (Fig. 2K).

(See figure on next page.)

Fig. 1 LINC01116 interacts with the SL1 components. **A** Computational prediction indicating LINC01116 interaction with SL1 components TAF1A and TAF1D. **B** and **C** Gene Set Enrichment Analysis showing enrichment of LINC01116 expression in ribosome biogenesis and rRNA metabolic processes in LUAD. **D** qPCR analysis reveals a significant positive correlation (Pearson) between LINC01116 and 47S rRNA expression, n = 6). **E** and **F** qPCR data demonstrating the stable overexpression of LINC01116 or stable knockdown of LINC01116 in A549 and H23 cells. **G** and **H** qPCR demonstrating relative enrichment of TAF1A or TAF1D in LINC01116 overexpression and knockdown cells. (**I** and **J**). Fluorescent in-situ hybridization images showing the co-localization of LINC01116 with NPM1, TAF1A, and TAF1D in LINC01116 overexpression cells or LINC01116 knockdown cells. **K** Schematic representation of immunoprecipitation of rDNA-bound SL1 complex. **L** Immunoblot analysis of SL1 complex immunoprecipitated from rDNA-promoter-bound chromatin. TAF1A-D subunits are detected, confirming successful SL1 complex isolation. (**M** and **N**). qPCR data confirming the relative enrichment of rDNA core promoter and LINC01116 after rDNA-bound SL1 immunoprecipitation. *P ≤ 0.05, **P ≤ 0.005, ***P ≤ 0.0005, ****P ≤ 0.00005. Error bars indicate mean ± SEM. NPM1, Nucleophosmin 1

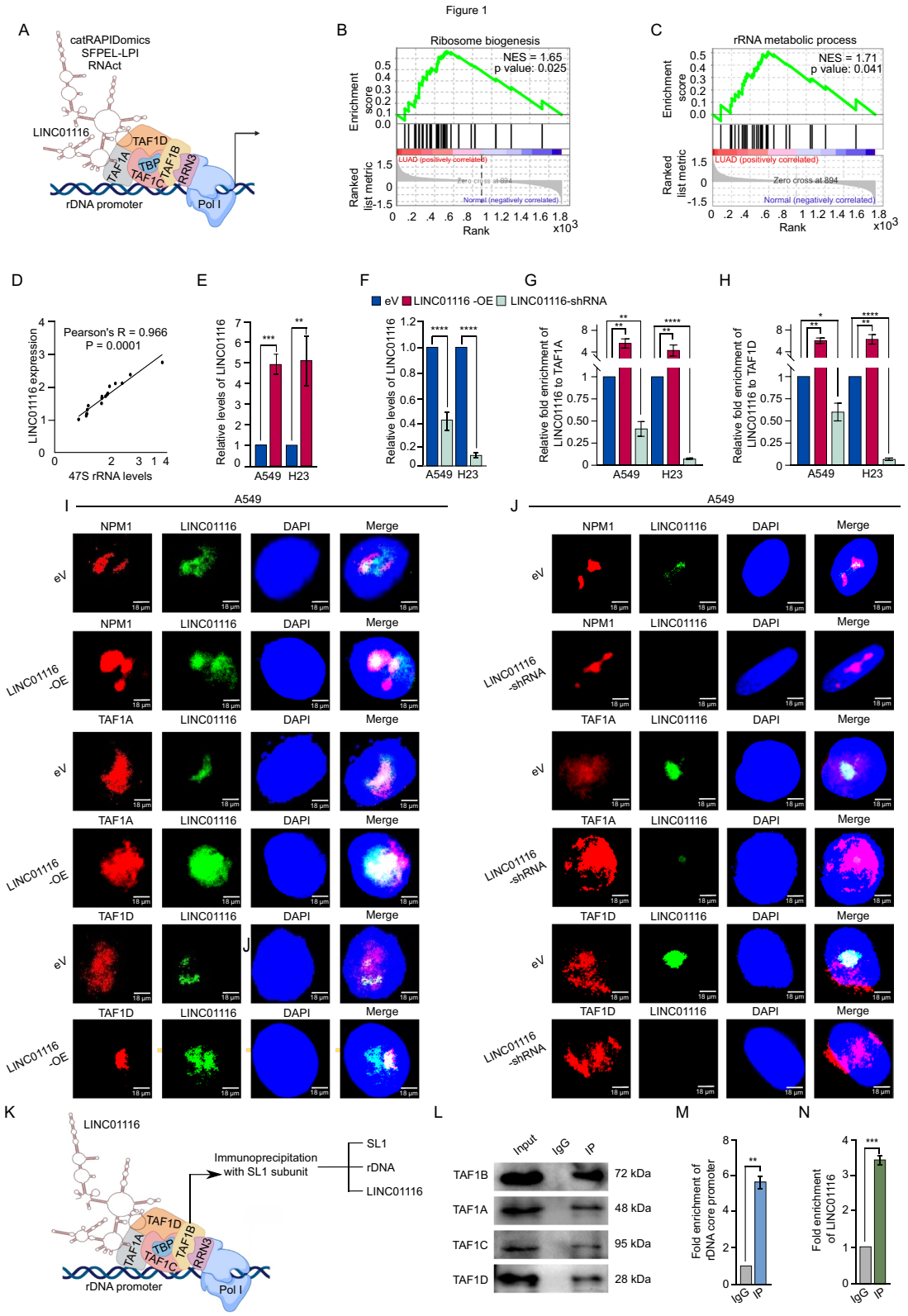

Fig. 1 (See legend on previous page.)

Serum starvation dampens Pol I transcription, resulting in reduced rRNA synthesis; this effect can be reversed upon serum reconstitution [35]. To study the involvement of LINC01116 in stimulus-mediated activation of Pol I transcription, cells with LINC01116 overexpression or knockdown were subjected to serum starvation, and rRNA de novo synthesis was measured. As anticipated, serum deprivation significantly decreased rRNA synthesis, as evidenced by reduced EU incorporation. However, upon serum re-stimulation, LINC01116-overexpressing cells exhibited a notable increase in rRNA levels, exceeding basal levels (Fig. 2L). Conversely, LINC01116 knockdown cells displayed impaired Pol I transcriptional reactivation upon serum reconstitution (Fig. 2M). Collectively, these findings strongly establish a positive regulatory role of LINC01116 on Pol I transcription.

LINC01116-driven Pol I transcription is essential for enhanced cell proliferation, clonogenicity and reduced apoptosis

Given that hyperactive Pol I transcription drives malignant proliferation [36], and LINC01116 upregulation is associated with increased proliferation in various cancers [37–39], we investigated the plausible link between LINC01116 and Pol I transcription controlling cell proliferation. We administered the specific Pol I inhibitor BMH-21 [40] to cells with either overexpression or knockdown of LINC01116 and assessed cell proliferation. Overexpression of LINC01116 resulted in a significant increase in cell proliferation, which was substantially reduced by BMH-21 treatment relative to controls. Conversely, in LINC01116 knockdown cells, BMH-21 treatment caused a further decrease in cell proliferation compared to the effect of knockdown alone (Fig. 3A). To further investigate the combined effects of BMH-21 treatment and LINC01116 knockdown on cell viability, we performed a dose–response analysis in A549 and H23 cells stably expressing shRNA-LINC01116. As shown in Fig. 3B, LINC01116 knockdown significantly potentiated the anti-proliferative effects of BMH-21 treatment, resulting in a synergistic decrease in cell viability in both cell lines. Tumor spheroids closely mimic in vivo tumors, and provide a more realistic environment for studying cell proliferation [41]. We generated tumor spheroids from A549 and H23 cells stably overexpressing LINC01116 or LINC01116-shRNA (Fig. 3C). LINC01116-overexpressing spheroids exhibited increased rRNA synthesis, while LINC01116-shRNA spheroids showed reduced rRNA levels, as measured by EU incorporation. Notably, BMH-21 treatment reduced rRNA levels in LINC01116-overexpressing spheroids and caused a synergistic decrease in rRNA transcription in LINC01116 knockdown spheroids (Fig. 3D). In addition, LINC01116 overexpressing spheroids also displayed higher Ki67 expression, a proliferation marker, compared to controls, while knockdown spheroids had reduced Ki67 expression. BMH-21 significantly decreased Ki67 levels in LINC01116-overexpressing spheroids, with an even greater reduction in knockdown spheroids (Fig. 3E). These results indicate that LINC01116 promotes cell proliferation through Pol I transcription. Further, BMH-21 treatment had a marginal effect on the clonogenic capacity of A549 and H23 cells overexpressing LINC01116. In contrast, LINC01116 knockdown cells exhibited a significant reduction in clonogenicity upon BMH-21 treatment. Notably, reconstitution of LINC01116 in knockdown cells rescued the clonogenic capacity (Fig. 3F). The rate of Pol I transcription is closely linked to cell cycle progression [42]. To investigate whether LINC01116-mediated Pol I transcription influences cell cycle dynamics, we analyzed the cell cycle distribution in LINC01116-overexpressing, knockdown or reconstituted cells. LINC01116 overexpression resulted in a significant decrease in G1-phase and an increase in the S-phase population, whereas knockdown of LINC01116 increased G1 and reduced the S-phase population. Notably, treatment with the Pol I inhibitor BMH-21 caused G1 arrest and diminished

(See figure on next page.)

Fig. 2 LINC01116 upregulates Pol I transcription. (**A** and **B**). ChIP-qPCR data showing the relative promoter occupancy of PIC components after LINC01116 overexpression or, after LINC01116 knockdown. **C** Sequence alignment showing complementarity between LINC01116 and rDNA promoter. **D** and **E** Chromatin isolation by RNA purification-qPCR data confirming the relative binding of LINC01116 to the rDNA promoter in LINC01116 overexpressing cells, (**F** and **G**). in LINC01116 knockdown cells. **H** Sanger sequencing histogram confirming ChIRP DNA as rDNA promoter. **I.** qPCR analysis showing relative expression levels of LINC01116 in cells with stable overexpression (OE), knockdown (shRNA), and reconstitution (shRNA + OE) of LINC01116. **J** qPCR analysis showing changes in 47S rRNA expression levels in cells with stable LINC01116 overexpression, knockdown, and reconstitution. **K** EU incorporation assay illustrating changes in Pol I transcriptional activity in cells with LINC01116 overexpression, knockdown, and reconstitution. Bar graphs illustrating the normalized fluorescence intensity. **L** EU incorporation assay demonstrating enhanced Pol I transcription in LINC01116 overexpression cells following serum reconstitution. **M** EU incorporation assay showing reduced Pol I reactivation in LINC01116 knockdown cells after serum reconstitution. Error bars indicate mean ± SEM. *P ≤ 0.05, **P ≤ 0.005,***P ≤ 0.0005, ****P ≤ 0.00005, #P ≤ E-7, ##P ≤ E-8. rDNA, ribosomal DNA, UCE, Upstream control element, EU, Ethynyl Uridine

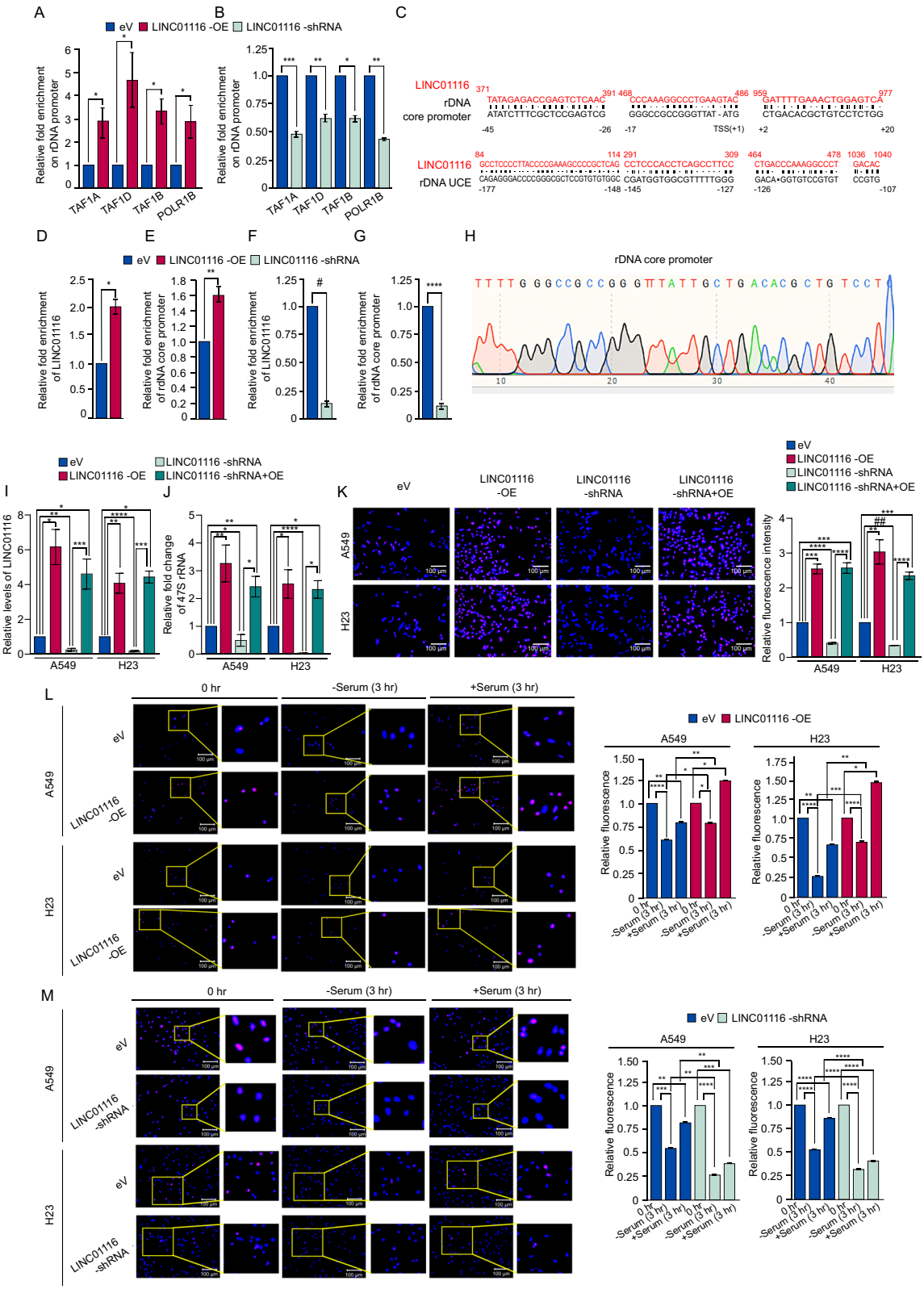

Fig. 2 (See legend on previous page.)

the S-phase enrichment observed in LINC01116-overexpressing cells. Additionally, BMH-21 treatment further decreased the S-phase population in LINC01116 knockdown cells, suggesting a synergistic effect. Moreover, reconstitution of LINC01116 expression in knockdown cells substantially rescued the cell cycle phenotype, mitigating the G1-phase accumulation and S-phase depletion induced by LINC01116 depletion, in both control and BMH-21-treated conditions (Fig. 3G, and Additional file 7, Figure S4A and S4B). Cyclin-dependent kinases (CDKs) CDK2, CDK4, and CDK6 are key regulators of the G1 to S-phase transition [43, 44]. Remarkably, LINC01116 overexpression led to increased CDK2, CDK4, and CDK6 expression, which was reduced to basal levels upon BMH-21 treatment. Furthermore, BMH-21 treatment synergistically decreased the expression of these CDKs in LINC01116 knockdown cells. Notably, reconstitution of LINC01116 expression rescued CDK expression levels in knockdown cells with or without BMH-21 treatment. These results indicate that LINC01116 promotes cell cycle progression through upregulation of G1 to S-phase regulators in a Pol I transcription-dependent manner (Fig. 3H). LINC01116 has been shown to suppress apoptosis [38], and rRNA levels are inversely correlated with apoptosis [15]. To investigate the apoptotic link between LINC01116 and Pol I transcription, we treated A549 and H23 cells overexpressing or knocked down for LINC01116 with BMH-21 and performed apoptosis assays. Notably, LINC01116 overexpression significantly reduced apoptosis, while BMH-21 treatment only marginally increased apoptosis in these overexpressing cells. In contrast, BMH-21 treatment significantly augmented apoptosis in LINC01116 knockdown cells. In addition, reconstitution of LINC01116 expression in knockdown cells restored apoptotic resistance, rescuing cells from increased apoptosis in both untreated and BMH-21-treated conditions (Fig. 3I and Additional file 7: Fig. S4C and S4D).

Subsequently, we analyzed the expression of apoptotic markers in A549 and H23 cells with LINC01116 overexpression and knockdown and treated with BMH-21. qPCR analysis revealed that LINC01116 overexpression significantly decreased the expression of the apoptotic marker BAX, with BMH-21 treatment marginally increasing BAX expression in these cells. Conversely, BMH-21 treatment significantly upregulated BAX expression in LINC01116 knockdown cells. Additionally, BMH-21 treatment marginally decreased the anti-apoptotic marker Bcl2 in LINC01116 overexpression cells, while LINC01116 knockdown significantly reduced Bcl2 expression. Notably, reconstitution of LINC01116 in knockdown cells rescued BAX and Bcl2 expression changes (Fig. 3J). Overall, our results highlight the crucial role of heightened Pol I transcription in mediating the oncogenic effects of LINC01116 in LUAD cells.

Pol I transcription is essential for LINC01116-mediated EMT

Recent studies have linked Pol I transcription [8] and LINC01116 to EMT processes [45]. We investigated the effect of LINC01116-Pol I transcription interplay on cell migration and invasion. Remarkably, LINC01116 overexpression significantly increased cell migration, which was abrogated by inhibition of Pol I transcription by BMH-21 treatment. However, BMH-21 treatment had marginally reduced migration in LINC01116 knockdown cells. Notably, reconstituting LINC01116 expression in knockdown cells rescued the migratory phenotype (Fig. 4A). Furthermore, BMH-21 treatment significantly dampened the increased invasiveness of LINC01116-overexpressing cells, with an even more pronounced decrease in invasiveness observed in LINC01116 knockdown cells.

(See figure on next page.)

Fig. 3 LINC01116-driven Pol I transcription modulates cell proliferation, clonogenicity, and apoptosis. **A** Alamar blue cell proliferation assay showing decreased proliferation of A549 and H23 cells stably overexpressing LINC01116 or LINC01116-shRNA treated with BMH-21. **B** Dose–response curves illustrating enhanced sensitivity to BMH-21 in LINC01116 knockdown cells, demonstrating a synergistic effect on cell viability. **C** qPCR showing the expression of LINC01116 in tumor spheroids generated from A549 and H23 cells stably overexpressing LINC01116 or LINC01116-shRNA. **D** EU incorporation assay showing Pol I transcription levels in tumor spheroids stably overexpressing LINC01116 or LINC01116-shRNA with or without inhibiting Pol I transcription by BMH-21. **E** Immunofluorescence images showing increased Ki67 expression in tumor spheroids stably overexpressing LINC01116 or LINC01116-shRNA in response to Pol I transcription inhibition. **F** Representative images of clonogenic assays showing the effect of BMH-21 treatment on A549 and H23 cells stably overexpressing LINC01116 (OE), Knockdown of LINC01116 (shRNA) or Reconstituted LINC01116 expression in knockdown cells (shRNA + OE), bar graphs illustrating relative colony counts for each condition normalized to untreated controls. **G** Bar graphs showing G1, S, and G2/M phase distributions in LINC01116-overexpressing (OE), LINC01116-shRNA, and reconstituted LINC01116 expression (shRNA + OE) cells with or without BMH-21 treatment. **H** qPCRs showing altered expression of cell cycle regulators CDK2, CDK4, and CDK6 in BMH-21 treated cells stably overexpressing LINC01116,LINC01116-shRNA or reconstitution in knockdown cells. **I** Bar graphs showing the apoptosis percentage in BMH-21 treated A549 or H23 cells stably overexpressing, knockdown or reconstitution of LINC01116. **J.** qPCRs showing the expression of pro-apoptotic and anti-apoptotic gene expression in BMH-21 treated cells with stable LINC01116 overexpression, knockdown or reconstitution in LINC01116 knockdown cells. Data represented as mean ± SEM. *P ≤ 0.05, **P ≤ 0.005,***P ≤ 0.0005, ****P ≤ 0.00005, ###P ≤ E-9, $P ≤ E-11,$$P ≤ E-13

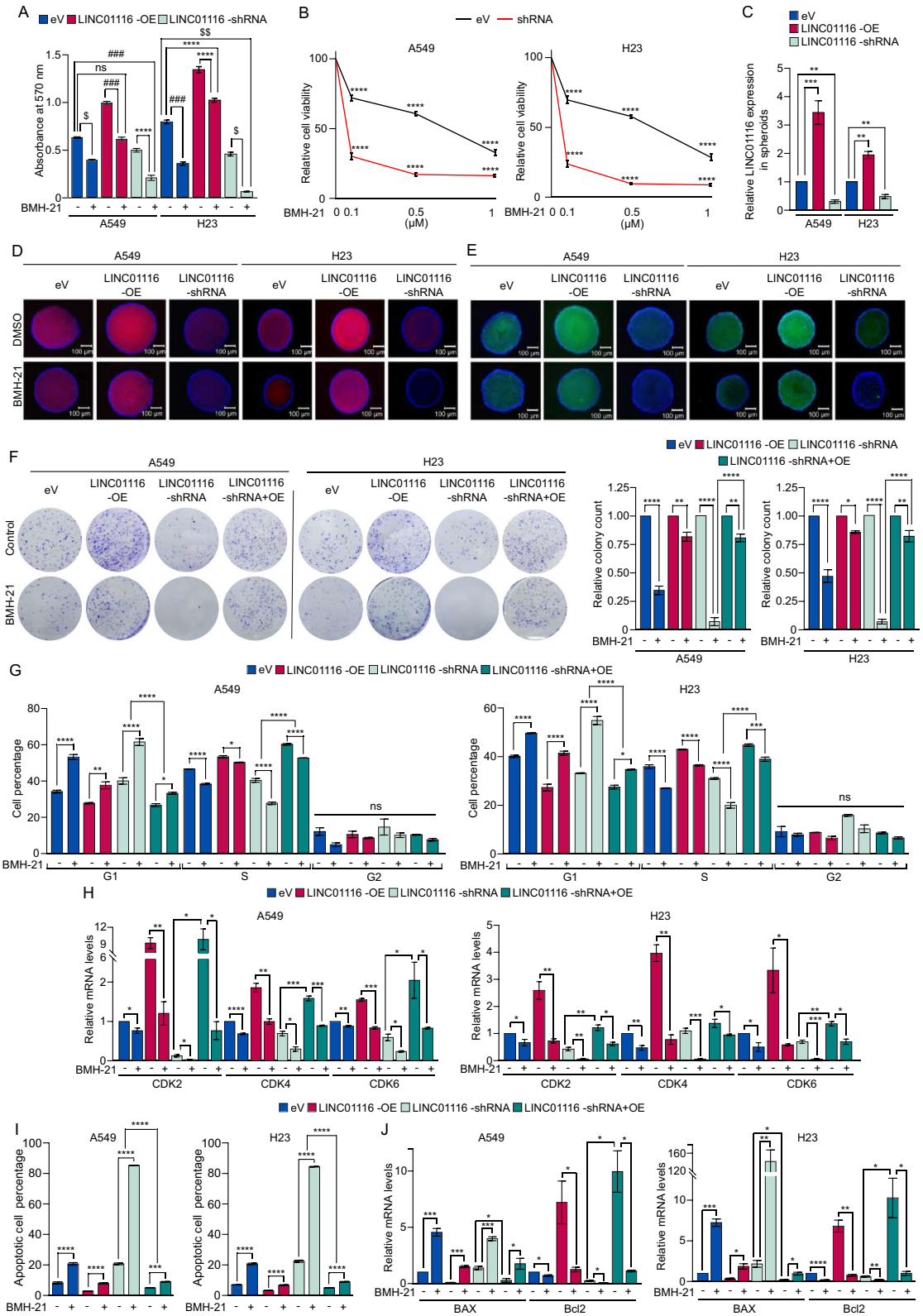

Fig. 3 (See legend on previous page.)

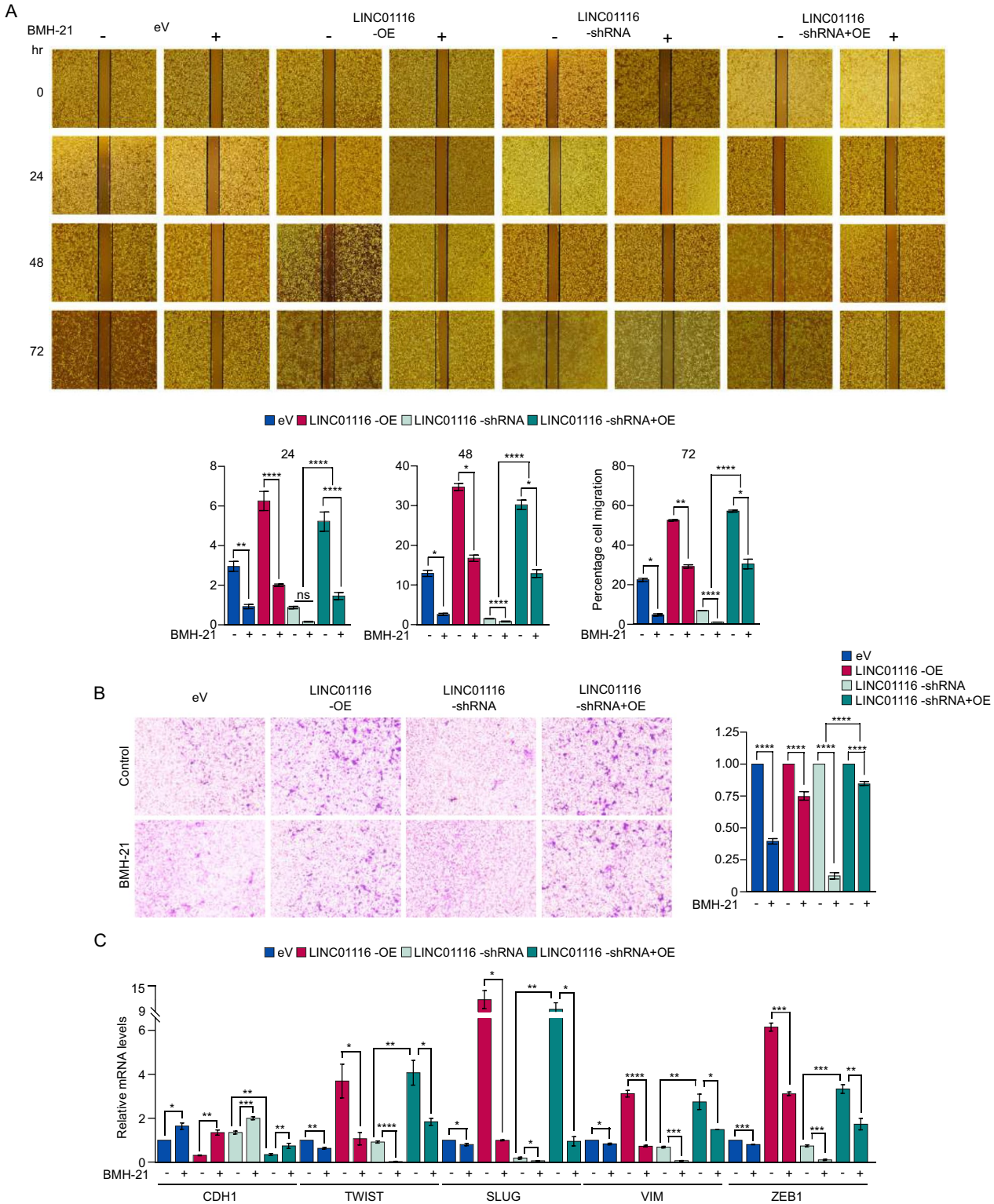

Fig. 4 Effect of LINC01116-mediated Pol I transcription on EMT. **A** Wound healing assay showing decreased cell migration in BMH-21 treated A549 cells with stable overexpression or knockdown of LINC01116, reconstitution of LINC01116 expression rescues migration defects, bar graphs indicate relative cell migration. **B** The trans-well invasion assay demonstrating reduced invasion of A549 cells with stable LINC01116 overexpression or knockdown, after BMH-21 treatment. LINC01116 reconstitution restores invasive capabilities, bar graphs illustrate relative cell invasion. **C** qPCR data of BMH-21 treated A549 cells with stable LINC01116 overexpression, knockdown or reconstitution showing changes in the EMT marker genes. Data represented as mean ± SEM. *P ≤ 0.05, **P ≤ 0.005,***P ≤ 0.0005, ****P ≤ 0.00005

Remarkably, reconstituted LINC01116 expression partially rescued the invasive phenotype in knockdown cells (Fig. 4B). These findings indicate that the LINC01116-Pol I transcription axis plays a crucial role in promoting cell migration and invasion potential of LUAD cells.

Upregulation of Pol I transcription promotes EMT by modulating the expression of key genes involved [15]. To investigate whether LINC01116-dependent upregulation of Pol I transcription alters the expression of genes essential for EMT, we treated LINC01116-overexpressing and knockdown cells with BMH-21 and evaluated the expression of EMT markers. Overexpression of LINC01116 reduced the expression of the epithelial marker CDH1, and BMH-21 treatment further repressed CDH1 expression compared to controls. Conversely, CDH1 expression was significantly upregulated in LINC01116 knockdown cells upon Pol I inhibition compared to controls. Moreover, LINC01116 overexpression significantly upregulated mesenchymal markers SLUG, TWIST, VIM, and ZEB1, which were markedly reduced upon BMH-21 treatment. In LINC01116 knockdown cells, BMH-21 treatment further significantly decreased the expression of mesenchymal markers. Notably, Reconstituting LINC01116 in knockdown cells rescued CDH1 downregulation, and restored SLUG, TWIST, VIM, and ZEB1 expression levels in knockdown cells (Fig. 4C). In summary, our data strongly indicate that Pol I transcription plays a crucial role in regulating LINC01116-mediated EMT in LUAD.

LINC01116 confers chemoresistance through upregulating Pol I transcription

Increased Pol I transcriptional activity [7] and LINC01116 expression [20] have been correlated to chemoresistance. To evaluate the mechanistic role of LINC01116-Pol I transcription in chemoresistance, we first treated A549 cells, either overexpressing LINC01116 or with LINC01116 knockdown, with Cis and Dox. LINC01116 knockdown significantly increased apoptosis in response to Cis and Dox, while LINC01116 overexpression reduced this effect, indicating the role of LINC01116 in modulating chemosensitivity (Fig. 5A, B, and Additional file 8: Figure S5A). Next, to investigate the

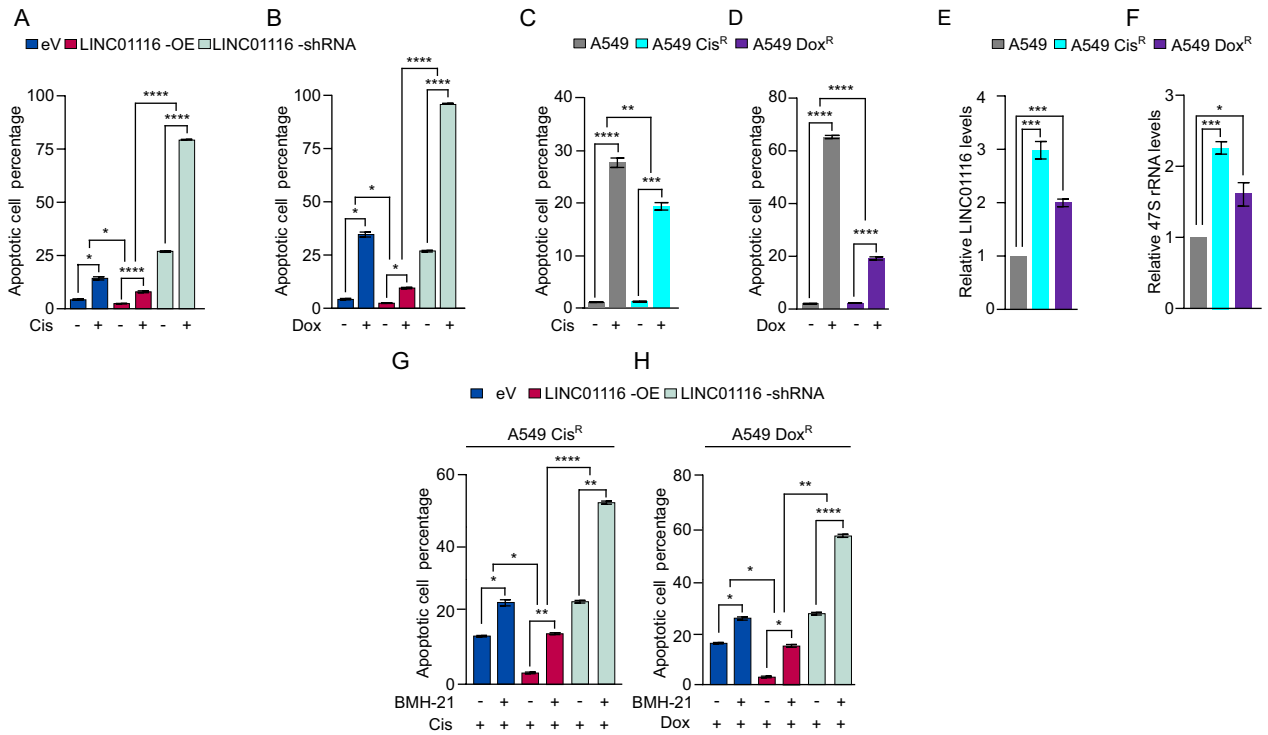

Fig. 5 LINC01116 contributes to chemoresistance through Pol I transcription. **A** and **B** Bar graph showing apoptosis percentage of Cis and Dox treated A549 cells with stable LINC01116 overexpression or knockdown. **C** Bar graph showing apoptotic cell percentage in Cis-treated A549 and A549-Cis^R cells. **D** Bar graph showing apoptotic cell percentage in Dox-treated A549 and A549-Dox^R cells. **E** qPCR data showing LINC01116 upregulation in A549-Cis^R and A549-Dox^R cells compared to A549 cells. **F** qPCR data showing upregulation of 47S rRNA in A549-Cis^R and A549-Dox^R cells compared to A549 cells. **G** Bar graph showing apoptotic cell percentage in the A549-Cis^R cells with overexpression or knockdown of LINC01116 and treated with BMH-21. **H** Bar graph showing apoptotic cell percentage in the A549-Dox^R cells overexpressing or knockdown of LINC01116 and treated with BMH-21. Data represented as mean ± SEM. *P ≤ 0.05, **P ≤ 0.005,***P ≤ 0.0005, ****P ≤ 0.00005. Cis, Cisplatin; Dox, Doxorubicin

impact of LINC01116-Pol I transcription on drug sensitivity, we generated A549 cells resistant to Cis or Dox. Flow cytometry demonstrated a significant decrease in sensitivity to Cis (Fig. 5C, Additional file 8: Figure S5B) and Dox (Fig. 5D, Additional file 8: Figure S5C) in the resistant cells compared to the parental A549 cells, indicating the gain of a resistant phenotype. Subsequently, we measured LINC01116 expression in these resistant cells. Interestingly, LINC01116 is upregulated in A549-Cis^R and A549-Dox^R cells compared to control A549 cells (Fig. 5E). Further, qPCR analysis revealed a significant increase in the expression of 47S rRNA levels in A549-Cis^R and A549-Dox^R cells, compared to control cells (Fig. 5F). Next, we overexpressed or knocked down the expression of LINC01116 in A549-Cis^R and A549-Dox^R cells growing in Cis or Dox respectively, with or without BMH-21, and evaluated apoptosis. Intriguingly, in A549-Cis^R cells, LINC01116 overexpression reduced cisplatin sensitivity and decreased apoptosis, whereas knockdown enhanced cisplatin sensitivity and increased apoptosis. Pol I inhibition with BMH-21 further augmented apoptosis in the knockdown group, while LINC01116-mediated Pol I upregulation reduced the apoptotic response to BMH-21 (Fig. 5G, and Additional file 8: Fig. S5D). Similarly, in A549-Dox^R cells. Overexpression of LINC01116 reduced doxorubicin sensitivity, while knockdown reversed this effect. Treating the transfected cells with BMH-21 resulted in a marginal increase in apoptosis. However, BMH-21 significantly augmented apoptosis in the LINC01116 knockdown group (Fig. 5H, and Additional file 8: Fig. S5E). These findings emphasize the pivotal role of LINC01116-mediated Pol I transcription in Cis and Dox response.

c-Myc transcriptionally activates LINC01116 expression

LINC01116 is upregulated in various cancers [45], but the underlying regulatory mechanisms are unclear. We identified putative c-Myc binding sites on the LINC01116 promoter at − 1 to − 48 bp upstream of the transcription start site (Fig. 6A). To investigate this, using transcriptomic data of LUAD on TCGA, we first performed a correlation analysis and found a significant positive correlation between c-Myc and LINC01116 expression (Fig. 6B). Notably, a significant positive correlation has been observed between c-Myc and LINC01116 expression LUAD tumors compared to normal (Fig. 6C).

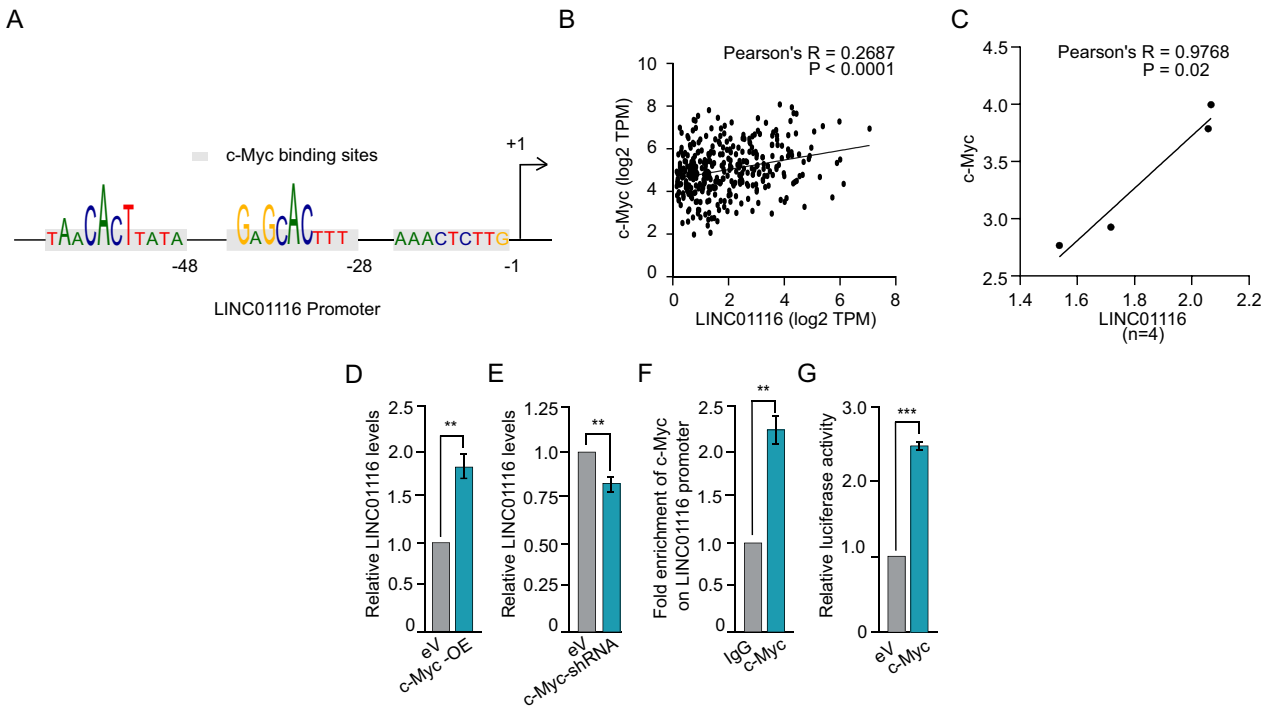

Fig. 6 c-Myc regulates LINC01116 expression. **A** Computational prediction demonstrating putative c-Myc binding sites on the LINC01116 promoter. **B** Correlation analysis using TCGA data showing a positive correlation between c-Myc and LINC01116 expression in LUAD. **C** QPCR validation in LUAD tumor tissues confirms a strong positive correlation between c-Myc and LINC01116 expression. **D** qPCR data illustrating LINC01116 upregulation with c-Myc overexpression. **E** qPCR data showing c-Myc knockdown downregulates LINC01116 expression. **F** ChIP-qPCR data showing significant enrichment of c-Myc on the LINC01116 promoter. **G** Luciferase assay data demonstrating the functional binding of c-Myc on the LINC01116 promoter. Data represented as mean ± SEM. **P ≤ 0.005,***P ≤ 0.0005

Furthermore, overexpression of c-Myc markedly upregulated LINC01116 expression (Fig. 6D), whereas shRNA-mediated c-Myc knockdown resulted in a marked decrease in LINC01116 levels (Fig. 6E) in A549 cells, indicating a transcriptional regulation of LINC01116 by c-Myc. In addition, we performed ChIP assays to validate the binding of c-Myc to the LINC01116 promoter. ChIP-qPCR with an anti-Myc antibody confirmed significant c-Myc enrichment on the LINC01116 promoter (Fig. 6F). To further validate this interaction, we transfected HEK293T cells with a luciferase reporter construct containing the LINC01116 promoter sequence along with either a c-Myc expression vector or an empty vector control. Remarkably, luciferase activity significantly increased upon c-Myc overexpression compared to the control, indicating specific c-Myc binding to the LINC01116 promoter and subsequent transcriptional activation (Fig. 6G). These findings confirm that c-Myc directly interacts with the LINC01116 promoter, driving its transcriptional activation in A549 cells.

Discussion

Hyperactive Pol I transcription is recognized as a canonical molecular aberration linked to various cancer hallmarks [46, 47]. Despite this, the precise molecular mechanisms driving this dysregulation remain elusive. Our study is the first to identify a novel regulatory pathway involving LINC01116, which drives the upregulation of Pol I transcription in LUAD. Importantly, this LINC01116-mediated upregulation of Pol I transcription plays a pivotal role in promoting various oncogenic processes, highlighting the significance of LINC01116-Pol I in the molecular etiology of LUAD.

Hyperactive Pol I transcription necessitates increased recruitment of pre-initiation complex (PIC) components to the rDNA promoter [35]. Our study shows that oncogenic LINC01116 operates as a scaffold, facilitating the assembly of essential transcription factors (TFs) at the rDNA promoter, critical for initiating rRNA synthesis. Previous studies have demonstrated that SLERT, a snoRNA-ended lncRNA, enhances pre-rRNA transcription by binding to the DEAD-box RNA helicase DDX21 and altering rDNA topology. Intriguingly, these findings connect SLERT-dependent regulation of Pol I transcription to ribosome biogenesis, underscoring the intricate regulatory networks linking Pol I transcription to ribosome biogenesis [48, 49]. Notably, lncRNA-TF scaffolding has also been observed to modulate Pol II-driven transcription by preventing the recruitment of Pol II or specific transcription factors. For example, the tumor-suppressor lncRNA GAS5, dysregulated in several cancers, promotes growth arrest, apoptosis, and inhibits cell migration by blocking the glucocorticoid receptor from binding to glucocorticoid response elements, thereby regulating target gene transcription [50, 51]. Intriguingly, lncRNA B2 RNA interacts with the Pol II σ-holoenzyme, preventing the assembly of a functional pre-initiation complex, and thereby suppressing Pol II transcription initiation [52]. Moreover, lncRNA–TF interactions have demonstrated both tumor suppressor and oncogenic roles in cancer. For instance, HAND2-AS1 binds E2F4 at the C16orf74 promoter to downregulate its expression and repress cervical cancer progression [53], whereas HNF1A-AS1 binds PBX3 to upregulate OTX1 expression, promoting angiogenesis in colon cancer [54]. These findings underscore the critical role of lncRNA-TF interactions in regulating transcription and their profound impact on cancer progression, highlighting their potential as therapeutic targets.

Recent studies have linked LINC01116 to promoting cell proliferation and cycle progression in cancer cells [55]. However, these studies predominantly explored the indirect effects mediated by microRNA-LINC01116 interactions. In this study, we uncover the direct impact of LINC01116 on cancer cell proliferation through the activation of Pol I transcription. Given that accelerated Pol I transcription is pivotal for malignant proliferation, LINC01116-dependent activation of Pol I transcription can be a potential target to reduce tumor burden. The rate of Pol I transcription is tightly coordinated with cell cycle progression to meet the varying demands for protein synthesis during different phases of the cell cycle [56]. Pol I transcription is moderately active during G1 phase and peaks as cells enter the S-phase, where the demand for protein synthesis is high [57]. We found that LINC01116-dependent activation of Pol I transcription is essential for driving cells into S-phase, indicating that LINC01116 plays a crucial role in facilitating cell cycle progression by ensuring sufficient rRNA synthesis to support heightened protein production needs during DNA replication. Elevated Pol I transcription promotes the synthesis and function of key cell cycle regulators, including cyclins, cyclin-dependent kinases (CDKs), and proteins involved in the Rb and p53 pathways [58, 59]. This process is tightly integrated with the functions of CDK2, CDK4, and CDK6, particularly during the S phase of the cell cycle. Our study indicates that LINC01116-mediated Pol I transcription upregulates CDK2, CDK4, and CDK6, highlighting a crucial mechanism that drives cell cycle progression. Interestingly, other oncogenic lncRNAs have similar roles. For example, SNHG6 promotes G1-S transition and proliferation in NSCLC cells. Additionally, MAFG-AS1 upregulates CDK2 expression via miR-339-5p

sponging, thereby accelerating the G1-S transition [60]. These findings underscore the importance of lncRNA-mediated regulation of cell cycle progression in cancer.

EMT initiation coincides with rDNA transcription activation, and inhibiting rRNA synthesis disrupts EMT and reduces metastasis [8]. Our recent findings demonstrate that miRNA-mediated inhibition of Pol I transcription significantly reduces A549 cell migration and downregulates ZEB1, a key EMT modulator [15]. Activation of Pol I transcription during EMT enhances ribosome biogenesis and protein synthesis, supporting the production of essential EMT proteins, including ZEB transcription factors. ZEB1 and ZEB2 repress epithelial markers and promote mesenchymal markers, stabilizing the mesenchymal state. This state requires continuous protein synthesis, maintained by Pol I activity. Our investigation revealed that LINC01116-dependent modulation of invasion and migration, and associated EMT markers expression requires activation of Pol I transcription. This interplay between Pol I and EMT mediated through LINC01116, highlights a critical juncture where Pol I activity governs the expression of crucial EMT regulators.

The association between Pol I transcription and chemoresistance is primarily due to hyperactive Pol I transcription driving proliferation, enhancing EMT processes, decreasing apoptosis, and activating survival pathways [7]. Our previous work showed that inhibiting Pol I transcription increased chemosensitivity in A549 cells [15]. In this study, we demonstrate that LINC01116-dependent upregulation of Pol I transcription reduces sensitivity to Cis and Dox, especially in drug-resistant cells. While LINC01116 role in chemoresistance has been linked predominantly to miRNA-dependent mechanisms [55], our findings suggest that increased Pol I transcription, facilitated by LINC01116, is a significant factor in chemoresistance.

Oncogenic c-Myc is a bona fide activator of Pol I transcription, directly binding to rDNA promoters, recruiting essential transcription factors, and enhancing rRNA synthesis [61]. This activation is considered a major oncogenic event in tumorigenesis. Our data suggests that c-Myc transcriptionally activates LINC01116 expression. Thus, c-Myc functions as an upstream regulatory node connecting both LINC01116 and Pol I transcription, creating a synergistic mechanism that drives crucial tumorigenic processes.

In summary, our study uncovers the critical link between oncogenic LINC01116 and Pol I transcription, offering valuable insights into the molecular basis of cancer pathogenesis. Also, highlights the intricate regulatory networks governing Pol I transcription in cancer.

Conclusion

In summary, our study reveals the synergistic role of LINC01116 and Pol I transcription in promoting oncogenic phenotypes in LUAD, including enhanced cell proliferation, clonogenicity, cell cycle progression, and chemoresistance, while suppressing apoptosis. The c-Myc-LINC01116-Pol I axis emerges as a crucial pathway in cancer development and progression, offering promising targets for therapeutic intervention. Our findings underscore the importance of lncRNA-mediated regulation of Pol I transcription and open new avenues for targeted cancer therapies aimed at disrupting this pathway to inhibit tumor growth and metastasis.

Abbreviations

CDKs	Cyclin-dependent kinases
ChIP	Chromatin Immunoprecipitation
ChIRP	Chromatin isolation by RNA purification
EMT	Epithelial-mesenchymal transition
EU	Ethynyl uridine
FISH	Fluorescence In-Situ hybridization
GSEA	Gene set enrichment analysis
LncRNAs	Long non-coding RNAs
LUAD	Lung Adenocarcinoma
PIC	Pre-Initiation Complex
Pol I	RNA Polymerase I
rDNA	Ribosomal DNA
RIP	RNA-Immunoprecipitation
rRNA	Ribosomal RNA
SL1	Selectivity factor 1
TBP	TATA binding protein
UBF	Upstream binding factor

Supplementary Information

The online version contains supplementary material available at https://doi.org/10.1186/s12967-024-05715-5.

Additional file 1: Table S1. List of primers, probes, and antibodies used in this study

Additional file 2: Figure S1. Computational predictions of lncRNAs interacting with Pol I proteome. A. Top four lncRNAs—LINC01116, LINC00471, LINC02449, and LINC00313 interacting with TAF1A and TAF1D, ranked by catRAPID star rating score. B. Box plots illustrating LINC01116, LINC00471, LINC02449, and LINC00313 expression levels in normal lung tissues and LUAD tumors from TCGA. C. Kaplan-Meier survival analysis of LINC01116, LINC00471, LINC02449, and LINC00313 expression in TCGA LUAD samples. Survival plots demonstrating significantly poorer survival in patients with high LINC01116 expression compared to low expression. FPKM, Fragments Per Kilobase of transcript per Million mapped reads

Additional file 3: Table S2. GSEA results summary for ribosome biogenesis

Additional file 4: Table S3. GSEA results summary for rRNA metabolic processes

Additional file 5: Figure S2. Interaction prediction between LINC01116 and TAF1A/TAF1D. A. catRAPID fragments histogram depicting the interaction profile between LINC01116 and TAF1A. B. Matrix showing the interaction predictions between LINC01116 nucleotides and TAF1A amino acids. C. catRAPID fragments histogram illustrating the interaction profile between LINC01116 and TAF1D. D. Interaction matrix showing the interaction predictions between LINC01116 nucleotides and TAF1D amino acids

Additional file 6: Figure S3: LINC01116 selectively binds to the rDNA UCE and core promoter regions. A. Schematic representation of the rDNA repeat. B. ChIRP-qPCR analysis demonstrating significant enrichment of

LINC01116 at the UCE and core promoter regions, with no significant changes in other regions

Additional file 7: Figure S4. Cell cycle and apoptosis analysis.. Flow cytometry histograms of cell cycle analysis of BMH-21 treated A549 and H23 cells stably overexpressing LINC01116,LINC01116-shRNA,or reconstitution of LINC01116 in knockdown cells.. Flow cytometry histograms of apoptosis assay of BMH-21 treated A549 and H23 cells stably overexpressing LINC01116,LINC01116-shRNA or reconstitution of LINC01116 in knockdown cells

Additional file 8: Figure S5. Apoptosis analysis in drug resistant cells. Flow cytometry histograms of apoptosis assay. A. Flow cytometry histogram of apoptosis assay of Cis and Dox treated A549 cells with stable LINC01116 overexpression or knockdown. B. Flow cytometry histograms of apoptosis assay of Cis-treated A549 or A549-Cis^R cells. C. Flow cytometry histograms of apoptosis assay of Dox-treated A549 or A549-Dox^R cells. D. Flow cytometry histograms of apoptosis assay of BMH-21 treated A549-Cis^R cells overexpressing or knockdown of LINC01116. E. Flow cytometry histograms of apoptosis assay of BMH-21 treated A549-Dox^R cells overexpressing or knockdown of LINC01116.

Acknowledgements
Thanks to Deepika Antil and Arpita Karmakar for the critical reading of the manuscript, Shivani Varshney for refining graphical abstract.

Author contributions
SSS acquired the data and drafted the manuscript. MS performed microscopy work, performed gene expression analysis and edited the manuscript. SS conducted computational analysis and contributed to manuscript editing. SN conceptualized, designed the study and drafted the manuscript.

Funding
This work is funded by Ramalingaswami early career fellowship – Department of Biotechnology and Indian Council of Medical Research (ICMR) awarded to SN.

Availability of data and materials
The data generated in the study is available in the manuscript and its supplementary data files.

Declarations

Ethics approval and consent to participate
Not applicable.

Consent for publication
All authors agreed to this publication.

Competing interests
The authors declare no competing interests.

Author details
[1]Department of Biomedical Engineering, Indian Institute of Technology Ropar, Rupnagar, Punjab, India.

Received: 31 July 2024 Accepted: 30 September 2024
Published online: 05 October 2024

References

1. Falcon KT, Watt KEN, Dash S, Zhao R, Sakai D, Moore EL, Fitriasari S, Childers M, Sardiu ME, Swanson S, et al. Dynamic regulation and requirement for ribosomal RNA transcription during mammalian development. Proc Natl Acad Sci USA. 2022;119: e2116974119.
2. Rossetti S, Wierzbicki AJ, Sacchi N. Mammary epithelial morphogenesis and early breast cancer. Evidence of involvement of basal components of the RNA polymerase I transcription machinery. Cell Cycle. 2016;15:2515–26.
3. Diesch J, Bywater MJ, Sanij E, Cameron DP, Schierding W, Brajanovski N, Son J, Sornkom J, Hein N, Evers M, et al. Changes in long-range rDNA-genomic interactions associate with altered RNA polymerase II gene programs during malignant transformation. Commun Biol. 2019;2:39.
4. Chen B, Huang Y, He S, Yu P, Wu L, Peng H. N(6)-methyladenosine modification in 18S rRNA promotes tumorigenesis and chemoresistance via HSF4b/HSP90B1/mutant p53 axis. Cell Chem Biol. 2023;30(144–158): e110.
5. Dolezal JM, Dash AP, Prochownik EV. Diagnostic and prognostic implications of ribosomal protein transcript expression patterns in human cancers. BMC Cancer. 2018;18:275.
6. Ueda M, Iguchi T, Nambara S, Saito T, Komatsu H, Sakimura S, Hirata H, Uchi R, Takano Y, Shinden Y, et al. Overexpression of transcription termination factor 1 is associated with a poor prognosis in patients with colorectal cancer. Ann Surg Oncol. 2015;22(Suppl 3):S1490-1498.
7. Cornelison R, Dobbin ZC, Katre AA, Jeong DH, Zhang Y, Chen D, Petrova Y, Llaneza DC, Steg AD, Parsons L, et al. Targeting RNA-polymerase I in both chemosensitive and chemoresistant populations in epithelial ovarian cancer. Clin Cancer Res. 2017;23:6529–40.
8. Prakash V, Carson BB, Feenstra JM, Dass RA, Sekyrova P, Hoshino A, Petersen J, Guo Y, Parks MM, Kurylo CM, et al. Ribosome biogenesis during cell cycle arrest fuels EMT in development and disease. Nat Commun. 2019;10:2110.
9. Goodfellow SJ, Zomerdijk JC. Basic mechanisms in RNA polymerase I transcription of the ribosomal RNA genes. Subcell Biochem. 2013;61:211–36.
10. Drygin D, Rice WG, Grummt I. The RNA polymerase I transcription machinery: an emerging target for the treatment of cancer. Annu Rev Pharmacol Toxicol. 2010;50:131–56.
11. Arabi A, Wu S, Ridderstrale K, Bierhoff H, Shiue C, Fatyol K, Fahlen S, Hydbring P, Soderberg O, Grummt I, et al. c-Myc associates with ribosomal DNA and activates RNA polymerase I transcription. Nat Cell Biol. 2005;7:303–10.
12. Cavanaugh AH, Hempel WM, Taylor LJ, Rogalsky V, Todorov G, Rothblum LI. Activity of RNA polymerase I transcription factor UBF blocked by Rb gene product. Nature. 1995;374:177–80.
13. Zhai W, Comai L. Repression of RNA polymerase I transcription by the tumor suppressor p53. Mol Cell Biol. 2000;20:5930–8.
14. Bywater MJ, Pearson RB, McArthur GA, Hannan RD. Dysregulation of the basal RNA polymerase transcription apparatus in cancer. Nat Rev Cancer. 2013;13:299–314.
15. Saproo S, Sarkar SS, Gupta E, Chattopadhyay S, Charaya A, Kalra S, Ahuja G, Naidu S. MiR-330-5p and miR-1270 target essential components of RNA polymerase I transcription and exhibit a novel tumor suppressor role in lung adenocarcinoma. Cancer Gene Ther. 2023;30:288–301.
16. Mattick JS, Amaral PP, Carninci P, Carpenter S, Chang HY, Chen LL, Chen R, Dean C, Dinger ME, Fitzgerald KA, et al. Long non-coding RNAs: definitions, functions, challenges and recommendations. Nat Rev Mol Cell Biol. 2023;24:430–47.
17. Wei C, Xu Y, Shen Q, Li R, Xiao X, Saw PE, Xu X. Role of long non-coding RNAs in cancer: from subcellular localization to nanoparticle-mediated targeted regulation. Mol Ther Nucleic Acids. 2023;33:774–93.
18. Liu W, Liang F, Yang G, Xian L. LncRNA LINC01116 sponges miR-93-5p to promote cell invasion and migration in small cell lung cancer. BMC Pulm Med. 2021;21:50.
19. Su X, Zhang J, Luo X, Yang W, Liu Y, Liu Y, Shan Z. LncRNA LINC01116 promotes cancer cell proliferation, migration and invasion in gastric cancer by positively interacting with lncRNA CASC11. Onco Targets Ther. 2019;12:8117–23.
20. Wang H, Lu B, Ren S, Wu F, Wang X, Yan C, Wang Z. Long noncoding RNA LINC01116 contributes to gefitinib resistance in non-small cell lung cancer through regulating IFI44. Mol Ther Nucleic Acids. 2020;19:218–27.
21. Lang B, Armaos A, Tartaglia GG. RNAct: protein-RNA interaction predictions for model organisms with supporting experimental data. Nucleic Acids Res. 2019;47:D601–6.
22. Zhang W, Yue X, Tang G, Wu W, Huang F, Zhang X. SFPEL-LPI: sequence-based feature projection ensemble learning for predicting LncRNA-protein interactions. PLoS Comput Biol. 2018;14: e1006616.
23. Bellucci M, Agostini F, Masin M, Tartaglia GG. Predicting protein associations with long noncoding RNAs. Nat Methods. 2011;8:444–5.

24. Gagliardi M, Matarazzo MR. RIP: RNA IMMUNOPRECIPITATION. Methods Mol Biol. 2016;1480:73–86.
25. Orjalo AV Jr, Johansson HE. Stellaris(R) RNA fluorescence in situ hybridization for the simultaneous detection of immature and mature long noncoding RNAs in adherent cells. Methods Mol Biol. 2016;1402:119–34.
26. Quinn JJ, Chang HY. In situ dissection of RNA functional subunits by domain-specific chromatin isolation by RNA purification (dChIRP). Methods Mol Biol. 2015;1262:199–213.
27. Naidu S, Shi L, Magee P, Middleton JD, Lagana A, Sahoo S, Leong HS, Galvin M, Frese K, Dive C, et al. PDGFR-modulated miR-23b cluster and miR-125a-5p suppress lung tumorigenesis by targeting multiple components of KRAS and NF-kB pathways. Sci Rep. 2017;7:15441.
28. Torres M, Becquet D, Guillen S, Boyer B, Moreno M, Blanchard MP, Franc JL, Francois-Bellan AM. RNA pull-down procedure to identify RNA targets of a long non-coding RNA. J Vis Exp. 2018. https://doi.org/10.3791/57379.
29. Chattopadhyay S, Sarkar SS, Saproo S, Yadav S, Antil D, Das B, Naidu S. Apoptosis-targeted gene therapy for non-small cell lung cancer using chitosan-poly-lactic-co-glycolic acid -based nano-delivery system and CASP8 and miRs 29A–B1 and 34A. Front Bioeng Biotechnol. 2023;11:1188652.
30. Feng Y, Zhang T, Zhang Z, Liang Y, Wang H, Chen Y, Yu X, Song X, Mao Q, Xia W, et al. The super-enhancer-driven lncRNA LINC00880 acts as a scaffold between CDK1 and PRDX1 to sustain the malignance of lung adenocarcinoma. Cell Death Dis. 2023;14:551.
31. Kurokawa R. Long noncoding RNA as a regulator for transcription. Prog Mol Subcell Biol. 2011;51:29–41.
32. Shang B, Li Z, Li M, Jiang S, Feng Z, Cao Z, Wang H. Silencing LINC01116 suppresses the development of lung adenocarcinoma via the AKT signaling pathway. Thorac Cancer. 2021;12:2093–103.
33. Zhao D, Liu W, Chen K, Wu Z, Yang H, Xu Y. Structure of the human RNA polymerase I elongation complex. Cell Discov. 2021;7:97.
34. Vance KW, Ponting CP. Transcriptional regulatory functions of nuclear long noncoding RNAs. Trends Genet. 2014;30:348–55.
35. James MJ, Zomerdijk JC. Phosphatidylinositol 3-kinase and mTOR signaling pathways regulate RNA polymerase I transcription in response to IGF-1 and nutrients. J Biol Chem. 2004;279:8911–8.
36. Ruggero D, Pandolfi PP. Does the ribosome translate cancer? Nat Rev Cancer. 2003;3:179–92.
37. Chen J, Yuan ZH, Hou XH, Shi MH, Jiang R. LINC01116 promotes the proliferation and inhibits the apoptosis of gastric cancer cells. Eur Rev Med Pharmacol Sci. 2020;24:1807–14.
38. Jiang L, Cheng C, Ji W, Wang H, Du Q, Dong X, Shao J, Yu W. LINC01116 promotes the proliferation and invasion of glioma by regulating the microRNA-744-5p-MDM2-p53 axis. Mol Med Rep. 2021. https://doi.org/10.3892/mmr.2021.12005.
39. Liang W, Wu J, Qiu X. LINC01116 facilitates colorectal cancer cell proliferation and angiogenesis through targeting EZH2-regulated TPM1. J Transl Med. 2021;19:45.
40. Jacobs RQ, Huffines AK, Laiho M, Schneider DA. The small-molecule BMH-21 directly inhibits transcription elongation and DNA occupancy of RNA polymerase I in vivo and in vitro. J Biol Chem. 2022;298: 101450.
41. Giusti I, Poppa G, D'Ascenzo S, Esposito L, Vitale AR, Calvisi G, Dolo V. Cancer three-dimensional spheroids mimic in vivo tumor features, displaying "inner" extracellular vesicles and vasculogenic mimicry. Int J Mol Sci. 2022. https://doi.org/10.3390/ijms231911782.
42. Grummt I. Life on a planet of its own: regulation of RNA polymerase I transcription in the nucleolus. Genes Dev. 2003;17:1691–702.
43. Fassl A, Geng Y, Sicinski P. CDK4 and CDK6 kinases: From basic science to cancer therapy. Science. 2022;375:eabc1495.
44. Honda R, Lowe ED, Dubinina E, Skamnaki V, Cook A, Brown NR, Johnson LN. The structure of cyclin E1/CDK2: implications for CDK2 activation and CDK2-independent roles. EMBO J. 2005;24:452–63.
45. Zeng L, Lyu X, Yuan J, Wang W, Zhao N, Liu B, Sun R, Meng X, Yang S. Long non-coding RNA LINC01116 is overexpressed in lung adenocarcinoma and promotes tumor proliferation and metastasis. Am J Transl Res. 2020;12:4302–13.
46. Grummt I. Wisely chosen paths–regulation of rRNA synthesis: delivered on 30 June 2010 at the 35th FEBS Congress in Gothenburg. Sweden FEBS J. 2010;277:4626–39.
47. Pelletier J, Thomas G, Volarevic S. Ribosome biogenesis in cancer: new players and therapeutic avenues. Nat Rev Cancer. 2018;18:51–63.
48. Wu M, Xu G, Han C, Luan PF, Xing YH, Nan F, Yang LZ, Huang Y, Yang ZH, Shan L, et al. lncRNA SLERT controls phase separation of FC/DFCs to facilitate Pol I transcription. Science. 2021;373:547–55.
49. Xing YH, Yao RW, Zhang Y, Guo CJ, Jiang S, Xu G, Dong R, Yang L, Chen LL. SLERT regulates DDX21 rings associated with Pol I transcription. Cell. 2017;169(664–678): e616.
50. Kino T, Hurt DE, Ichijo T, Nader N, Chrousos GP. Noncoding RNA gas5 is a growth arrest- and starvation-associated repressor of the glucocorticoid receptor. Sci Signal. 2010;3:ra8.
51. Pickard MR, Williams GT. Molecular and cellular mechanisms of action of tumour suppressor GAS5 LncRNA. Genes. 2015;6:484–99.
52. Espinoza CA, Allen TA, Hieb AR, Kugel JF, Goodrich JA. B2 RNA binds directly to RNA polymerase II to repress transcript synthesis. Nat Struct Mol Biol. 2004;11:822–9.
53. Gong J, Fan H, Deng J, Zhang Q. LncRNA HAND2-AS1 represses cervical cancer progression by interaction with transcription factor E2F4 at the promoter of C16orf74. J Cell Mol Med. 2020;24:6015–27.
54. Wu J, Meng X, Jia Y, Chai J, Wang J, Xue X, Dang T. Long non-coding RNA HNF1A-AS1 upregulates OTX1 to enhance angiogenesis in colon cancer via the binding of transcription factor PBX3. Exp Cell Res. 2020;393: 112025.
55. Xu Y, Yu X, Zhang M, Zheng Q, Sun Z, He Y, Guo W. Promising advances in LINC01116 related to cancer. Front Cell Dev Biol. 2021;9: 736927.
56. Russell J, Zomerdijk JC. RNA-polymerase-I-directed rDNA transcription, life and works. Trends Biochem Sci. 2005;30:87–96.
57. Klein J, Grummt I. Cell cycle-dependent regulation of RNA polymerase I transcription: the nucleolar transcription factor UBF is inactive in mitosis and early G1. Proc Natl Acad Sci U S A. 1999;96:6096–101.
58. Yuan X, Zhou Y, Casanova E, Chai M, Kiss E, Grone HJ, Schutz G, Grummt I. Genetic inactivation of the transcription factor TIF-IA leads to nucleolar disruption, cell cycle arrest, and p53-mediated apoptosis. Mol Cell. 2005;19:77–87.
59. Wang Q, Zhang W, Yin D, Tang Z, Zhang E, Wu W. Gene amplification-driven lncRNA SNHG6 promotes tumorigenesis via epigenetically suppressing p27 expression and regulating cell cycle in non-small cell lung cancer. Cell Death Discov. 2022;8:485.
60. Feng J, Wen T, Li Z, Feng L, Zhou L, Yang Z, Xu L, Shi S, Hou K, Shen J, et al. Cross-talk between the ER pathway and the lncRNA MAFG-AS1/miR-339-5p/ CDK2 axis promotes progression of ER+ breast cancer and confers tamoxifen resistance. Aging. 2020;12:20658–83.
61. Grandori C, Gomez-Roman N, Felton-Edkins ZA, Ngouenet C, Galloway DA, Eisenman RN, White RJ. c-Myc binds to human ribosomal DNA and stimulates transcription of rRNA genes by RNA polymerase I. Nat Cell Biol. 2005;7:311–8.

Publisher's Note